J Geophys (1984) 55:134-141

Journal of Geophysics

Ground-satellite coordinated study of the April 5, 1979 events: observation of O^+ cyclotron waves

B. Inhester [1], **U. Wedeken** [1], **A. Korth** [2], **S. Perraut** [3], **and M. Stokholm** [4]

[1] Institut für Geophysik der Universität Göttingen, D-3400 Göttingen, Federal Republic of Germany
[2] Max-Planck-Institut für Aeronomie, D-3411 Katlenburg-Lindau, Federal Republic of Germany
[3] Centre de Recherches en Physique de l'Environnement, CNET F-92131 Issy-les-Moulineaux, France
[4] Physikalisches Institut der Universität Bern, CH-3012 Bern, Switzerland

Abstract. In a period of particularly large magnetospheric disturbance, large amplitude pc2 waves were observed in the late dawn sector on GEOS-2 and in the vicinity of the foot-point of the satellite's field line. The waves have dominantly left-hand polarization and their frequency is closely correlated to the O^+ gyrofrequency in the magnetosphere. After the start of the pc2 activity, the GEOS-2 particle detectors measured an enhanced flux of energetic O^+ ions in the energy range from 0.9–16 keV. By calculating the dispersion of ion cyclotron waves in a multicomponent plasma, it is shown that the energetic O^+ ions can destabilize the observed pc2 waves.

Key words: Ion cyclotron waves - pc1-2 pulsations - Magnetospheric O^+ abundance

Introduction

During the last 5 years, the satellite missions of ATS-1 and 6 (Bossen et al., 1976; Mauk and McPherron, 1980) and of GEOS-1 and 2 (Gendrin et al., 1978; Young et al., 1981) have helped to identify the immediate neighbourhood of the magnetic equator in the magnetosphere as the emission region of the ground-observed pulsations in the pc1-2 frequency range. The energy source for most of these waves has been found to be the anisotropy of energetic H^+ ions (Roux et al., 1982; however see also Lanzerotti et al., 1983). Furthermore, it seems that the majority of the electromagnetic wave power generated at the magnetic equator in this frequency regime does not even reach the ionosphere (Perraut, 1982; Rauch and Roux, 1982; Perraut et al., 1984).

The presence of ions heavier than H^+ is frequently observed in the magnetosphere (e.g. Young, 1983) and by means of gyroresonant absorption, they subdivide the pc1-2 frequency regime into subranges between the gyrofrequencies of each ion species present. In satellite-observed wave spectra, the stop bands around the He^+ and O^+ gyrofrequency are clearly visible as gaps in the left-hand (LH) polarized mode (Fraser and McPherron, 1982; Mauk, 1983). Ray-tracing calculations of Rauch and Roux (1982) for a H^+, He^+ composition of the magnetosphere indicate that LH polarized ion cyclotron waves, with a frequency above the He^+ gyrofrequency at the equatorial plane of the magnetosphere, are converted into a right-hand (RH) polarized wave when they propagate along the field line towards the ionosphere. Subsequently, their frequency approaches the $H^+ - He^+$ hybrid resonance frequency and the waves are reflected back before they can reach the ground. The presence of O^+ ions in the magnetosphere will similarly prevent ion cyclotron waves in the frequency range between the O^+ and He^+ gyrofrequency penetrating from the equatorial plane to the ionosphere. Above a certain threshold of a few per cent for the He^+ and O^+ abundancy ratio, only waves having a frequency below the O^+ gyrofrequency are expected to reach the ground (Perraut et al., 1984).

The magnetosphere has been found to be particularily enriched with heavy ions after magnetically disturbed periods (Balsiger et al., 1980; Lennartsson et al., 1981). The present paper intends to relate pc2 pulsations observed on the ground after a series of substorms to simultaneous measurements from the GEOS-2 satellite. The frequency of the pulsations is below the O^+ gyrofrequency in the magnetosphere, which seems particularly favourable for a ground-satellite correlation. Furthermore, we will study the conditions for the generation of these low-frequency ion cyclotron waves with the help of the particle measurements from the GEOS-2 satellite.

Wave observations

The pc2 waves were observed in northern Scandinavia by the Göttingen magnetometer chain during the recovery phase of a series of substorms and 5 h after sudden commencement of another storm. Details of the general geophysical situation can be found in Wedeken et al. (1984). The amplitude of the pc2 waves that were recorded in the late dawn sector was unusually large with peak values of almost 5 nT at certain times. Figure 1 shows, as an example, part of the pulsation records from the almost north-south aligned chain of magnetometers (except for station ESR which is about 300 km west of IVA; see Fig. 3 or Wedeken et al., 1984, for details).

For a comparison with GEOS-2 data, we have reproduced the *H*-component magnetograms in compres-

Offprint requests to: B. Inhester

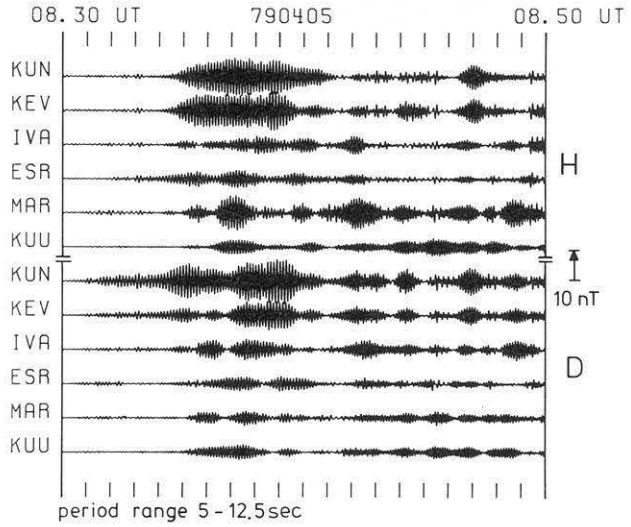

Fig. 1. Band-pass filtered pulsation records from April 5, 1979 in northern Scandinavia. For the location of the magnetometer stations see Fig. 3

sed form in Fig. 2. Above the magnetograms, we have plotted the ULF spectrogram, that was measured simultaneously on board GEOS-2, for LH polarized electromagnetic waves. Since the frequency of the pc2 pulsations as observed on the ground was 0.12–0.17 Hz, their counterpart in the GEOS-2 spectrogram has to be sought at the very bottom. For clarity, the power spectral density of these waves, integrated from 0.1–0.2 Hz, is drawn below the spectrogram. Comparing the temporal variation of the wave activity at GEOS-2 with the ground observations in the lower half of Fig. 2, the most obvious similarity is the absence of waves from 7:40–8:30 UT in both the satellite- and the ground-measured traces. We can also relate the large-amplitude wave packet observed on the ground just after 8:30 UT to a simultaneous wave emission of well-defined frequency at GEOS-2. Similar wave packets observed on the ground around 7:10 UT do not show up so clearly in the ULF spectrum, while the increase of the spectral width of the ULF waves after 7:30 UT apparently corresponds to a more irregular enhancement of the pc2 activity on the ground at the same time.

The relatively large pc2 waves seen on the ground around 7:10 UT do not seem to have been in conjunction with GEOS-2. We note that these particular pulsations are also absent in the ESR magnetogram and, therefore, seem to be highly localized. During quiet conditions, the foot-point of the GEOS-2 field line lies to the west of the magnetometer chain (see Wedeken et al., 1984), but at the time when the observations were made, the magnetosphere was heavily disturbed, thus making determination of the exact foot-point impossible. From the above observations, however, we conclude that the foot-point still lies to the west of the magnetometer chain, with ESR probably the nearest magnetometer station. This may become different towards the end of the record in Fig. 2, when GEOS-2 approached the magnetosheath and encountered strong broadband ULF bursts at 9:15 UT.

In order to demonstrate that the pc2 wave packets at around 7:10 UT are indeed localized, we have plot-

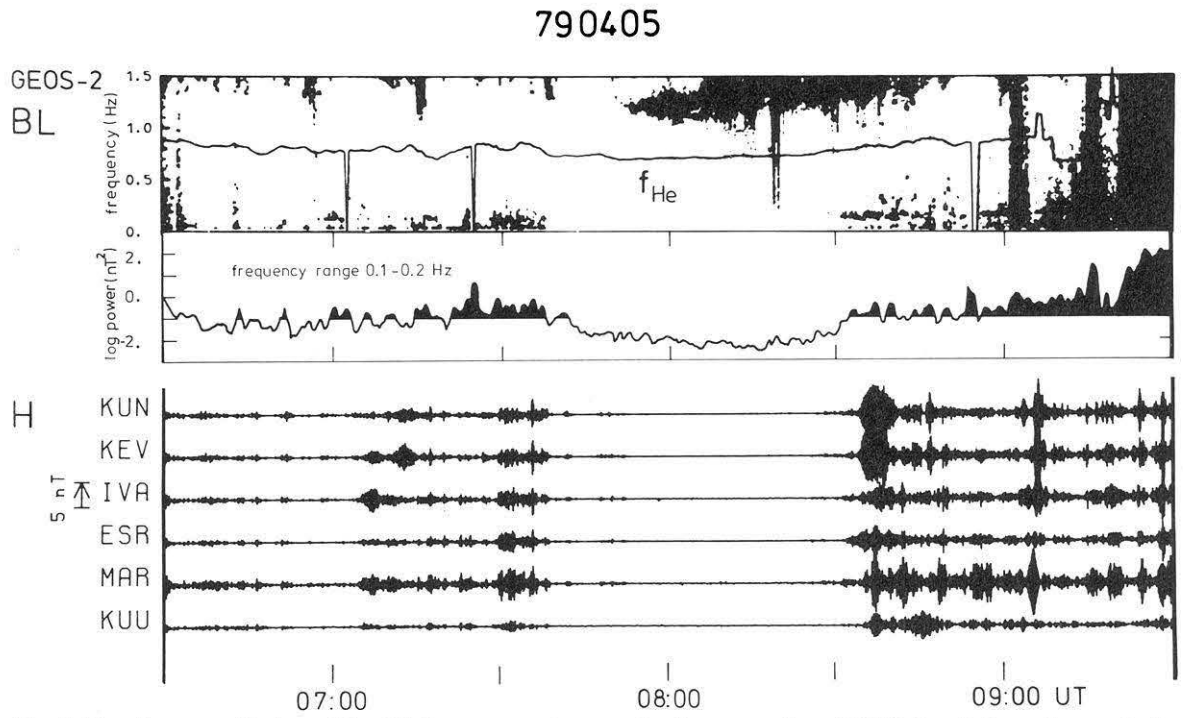

Fig. 2. Simultaneous display of the ULF wave spectrogram (*top*) measured on GEOS-2 and the pc2 records (*bottom*) seen on the ground. The spectrogram shows the intensity of the LH polarized component above a threshold value (1.80 $(nT)^2$/Hz at 1 Hz) as a black area in the frequency-time domain; the He^+ gyrofrequency is drawn as reference. Below the spectrogram, we show the temporal evolution of the integral over the power spectral density from 0.1–0.2 Hz. For clarity, we have blackened the area below the curve above the value of 0.1 nT^2. The ground measured records show the amplitudes of the *H*-component in the frequency range 0.08–0.2 Hz

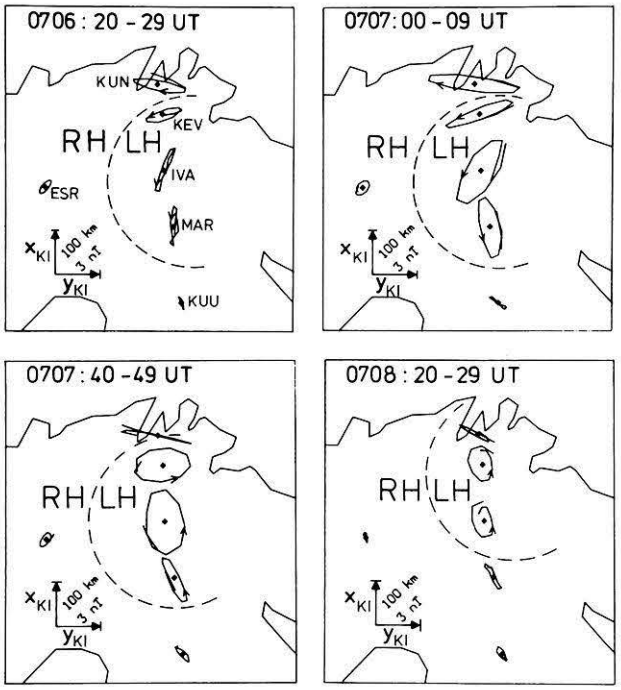

Fig. 3. Time sequence of hodograms for one of the pc2 wave packets. Here, a horizontal magnetic perturbation of 3 nT corresponds to a spatial distance of 100 km. The *dashed line* indicates the transition between the RH and LH sense of polarization. The latter clearly dominates the maximum region which seems to move slowly northward

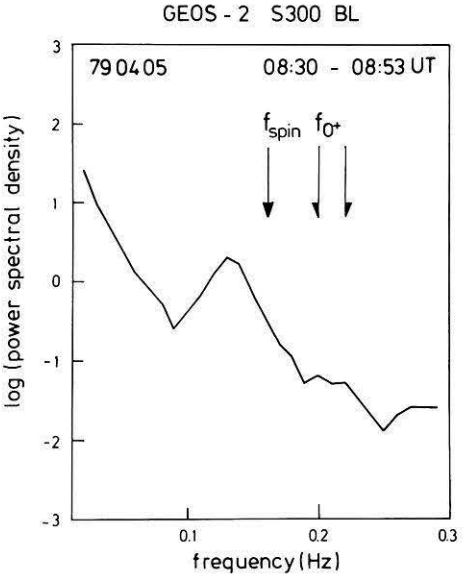

Fig. 4. Power spectrum derived by integration of the LH component intensities of the ULF wave spectrogram from 8:30–8:53 UT. The spectrum peaks at 0.13 Hz clearly different from the satellite's spin frequency at 0.16 Hz

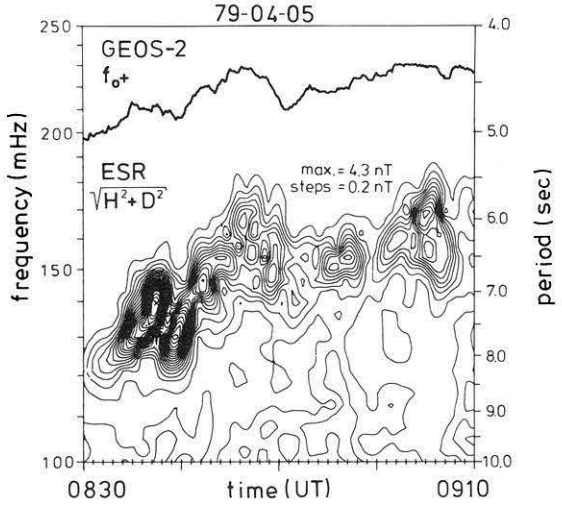

Fig. 5. Dynamic spectrum of the total horizontal magnetic perturbation at ESR from 8:30–9:10 UT. The contour lines are drawn for constant amplitude values 0.2 nT apart. For reference, the O^+ gyrofrequency at GEOS-2 is superposed. Note its close correlation with the spectral amplitude contour lines

ted a sequence of hodograms for one of the wave packets in Fig. 3. The maximum intensity of the wave packet is apparently concentrated on the magnetometer chain, or to the east of it. The figure also reveals that the wave packet is essentially LH polarized, as is expected for an ion cyclotron wave. The predominance of LH polarization was a general feature of the pc2 waves observed on the ground. Only during the more irregular emissions, e.g. after 7:30 UT, considerable RH polarization was also observed. These emissions also appeared less localized and were found as pi1 activity in the magnetograms of the IGS stations nearly 1500 km further west (H. Gough and C.A. Green, personal communication) and of the magnetometer station KST about 2000 km to the south.

Basically, the ULF wave experiment on board GEOS-2 has some difficulty in detecting wave energy in the pc2 frequency range below 0.2 Hz because of the interference with the satellite spin frequency at about 0.16 Hz. Since the satellite rotates in the RH sense, the interference only affects the RH component of the wave measurements, where it is suppressed by a notch filter (see Perraut et al., 1978, for details). That the pc2 waves we are presently concerned with can clearly be identified in the GEOS-2 wave spectrum is demonstrated in Figs. 4 and 5. The former shows the power spectral density in the LH polarized mode integrated over almost half an hour during the second period of pc2 activity starting at 8:30 UT. The peak in the power density at 0.13–0.14 Hz is clearly related to the ground-measured pulsations, as can be seen from a comparison with Fig. 5, which shows a dynamic spectrum of the ESR magnetogram for the same time period. Here, the frequency of the maximum amplitude increases slightly from 0.13–0.17 Hz. However, if the spectral amplitudes were integrated over the interval from 8:30–9:00 UT, the intensification at the beginning of the time period would also result in a maximum at a frequency of about 0.14 Hz.

On the dynamic spectrum in Fig. 5 we have superimposed the variation of the O^+ gyrofrequency, f_{O^+}, that corresponds to the ambient magnetic field measured in the vicinity of GEOS-2. The spectral power density of the ground-observed pulsations is entirely concentrated below f_{O^+} and the highest visible pc2

frequency f_{m2} shows a temporal variation closely following that of f_{O^+}. If we define f_{m2} by the uppermost contour line of the dynamic spectral plot, then the ratio f_{m2}/f_{O^+} varies between 0.65 and 0.80. These relations between the pulsation frequency and f_{O^+} hold equally well for the pc2 pulsations observed earlier between 7:00 and 7:30 UT, except for the more irregular emissions.

The fact that the pulsation frequency is controlled by the strength of the ambient magnetic field leads us to suspect that we are dealing with ion cyclotron waves. Also, the relatively narrow spectral bandwidth apparent in Fig. 5 is typical for these waves. The pc2 pulsations observed on the ground represent, however, only the low-frequency part of a sequence of ion cyclotron wave bands. In the frequency range between the gyrofrequencies f_{He^+} and f_{H^+} of helium and hydrogen ions, ion cyclotron waves were almost continuously recorded on board GEOS-2 from 6:00–9:00 UT with a major gap from 7:40 to 7:50 UT, when pc2 waves were also absent. In the spectrogram of Fig. 2, the reappearance of the ion cyclotron waves above f_{He^+} can be seen at 7:52 UT, at a frequency of 1.2 Hz. The polarization of these pc1 waves is almost linear, rather than in the LH sense, and at certain times the RH component even dominates. The ratio f_{m1}/f_{H^+} of the highest visible pc1 frequency, f_{m1}, with f_{H^+} varies between 0.4 and 0.7, where the smaller values are observed before 7:00 UT and from 7:50–8:30 UT, when the pc2 activity was absent. These pc1 waves were not observed on the ground in northern Scandinavia (T. Bösinger, personal communication), which can be understood from the results of Rauch and Roux (1982) and Perraut et al. (1984), if, in addition to H^+, the presence of heavier ions in the magnetosphere is assumed.

Model for the pc2 generation

The results of the GEOS-1 and 2 observations obtained so far clearly show that not only the propagation of ion cyclotron waves, but also their generation is greatly influenced by the ion composition of the magnetospheric plasma (Young et al., 1981; Roux et al., 1982). This is in accordance with the linear theory for waves in a homogeneous multiple ion plasma (e.g. Cupermann, 1981; Gendrin, 1981). If we assume quasineutrality of the plasma, cold electrons, and a wave vector **k** parallel to the ambient magnetic field, the dispersion relation for the ion cyclotron waves is, in conventional notation:

$$D(\omega,\mathbf{k})=k^2-\left(\frac{\omega}{c_0}\right)^2 + \sum_s \left(\frac{\omega_{ps}}{c_0}\right)^2 \left[\frac{\omega}{\Omega_s}+\frac{1}{2}\int d^3v \frac{v_\perp}{v_\parallel-(\omega-\Omega_s)/k} \cdot \left(\left(\frac{\omega}{k}-v_\parallel\right)\frac{\partial}{\partial v_\perp}+v_\perp\frac{\partial}{\partial v_\parallel}\right) g_s\right]. \quad (1)$$

Here, Σ_s sums over the ion species and ω_{ps}, Ω_s, g_s are their plasma and gyrofrequency (in: s^{-1}) and normalized velocity distribution, respectively. For growth rates $|\mathrm{Im}\,\omega| \ll |\mathrm{Re}\,\omega|$ the instability of the wave is essentially determined by the imaginary part (see Cornwall, 1965; Gendrin, 1981)

$$\mathrm{Im}\,D=-\pi\frac{\omega}{k}\sum_s\left(\frac{\omega_{ps}}{c_0}\right)^2\int dv_\perp^2\left(1+\frac{1}{2}\frac{v_\perp k}{\omega}\frac{\partial}{\partial\alpha}\right) g_s|_{v_\parallel=\frac{\omega-\Omega_s}{k}} \quad (2)$$

with a positive sign for Im D meaning instability, Here, α is the pitch angle and the velocity integration has to be carried out over the resonant plane $v_\parallel=(\omega-\Omega_s)/k$ in phase space. The first term of the integrand leads to an absorption of wave energy proportional to the number of particles in the resonant plane, whereas an instability can only be caused by the second term of the integrand if $\partial g_s/\partial\alpha$ becomes negative and cancels the first term.

For frequencies sufficiently different from any gyrofrequency, only energetic particles can make a significant contribution to Eq. (2). So far, only one sort of energetic ions, namely H^+, has been considered in the literature. In this case, a growth of ion cyclotron waves which propagate at $\omega<\Omega_{H^+}$ can only be achieved if $\partial g/\partial\alpha<0$ at $v_\parallel<0$, e.g. for a positive temperature anisotropy $(T_\perp/T_\parallel)-1$.

The particle data measured on board GEOS-2 on April 5, however, show a large enhancement of energetic O^+ besides H^+. Figure 6 shows the ion flux $J_\perp$ for an aspect angle $\alpha=90°$ immediately before and after the start of the pc2 activity, as derived from the ion composition experiment (S-303; energy $E<16$ keV/e; Geiss et al., 1978) and the charged particle spectrometer (S-321; $E>27$ keV/e; Korth et al., 1978). Before 7:00 UT H^+ is the dominant energetic ion, but between 7:07 UT and 7:20 UT a change in the energetic ion composition occurs with reduced H^+-fluxes, and O^+ as a second sort of energetic ions. The temporal development of the equivalent ion number densities in the energy range of 0.9–16 keV is shown in Fig. 7. After the enhancement of the O^+ density and the decrease of H^+ at about 7:10 UT, the ion densities in this energy range remained fairly constant until 9:15 UT when, due to encounters of GEOS-2 with the magnetosheath, large fluctuations of the particle fluxes were measured. The effect of additional energetic O^+ ions can easily be estimated from Eq. (2). If their anisotropy is positive, they help to destabilize ion cyclotron waves with a frequency below f_{O^+}, whereas they contributes to a damping of ion cyclotron waves above f_{O^+}. This is qualitatively what we observe in the ULF spectrum in Fig. 2.

In order to estimate quantitatively the possibility of ion cyclotron wave generation below f_{O^+}, we solved the dispersion relation (1) numerically. The ion distribution functions g_s were assumed bi-Maxwellian for each species, namely energetic H^+ and O^+ and cold H^+, O^+ and He^+. The Maxwell distributions were fitted to the ion flux measurements by use of the relation

$$\frac{J_{\perp s}(E)}{E}=\frac{2}{m_s^2}\left(1.6\cdot10^{-12}\,\frac{\mathrm{erg}}{\mathrm{eV}}\right)^2 g_s(v_\parallel=0,v_\perp)$$

where the energy E must be inserted in eV, the flux $J_\perp$ in (cm^2 strd s eV)$^{-1}$ and the ion mass m_s anf g_s in cgs-units. The anisotropy of the distribution function for energetic H^+ can be estimated from the pitch-angle dependence of the ion flux that was measured by the S-

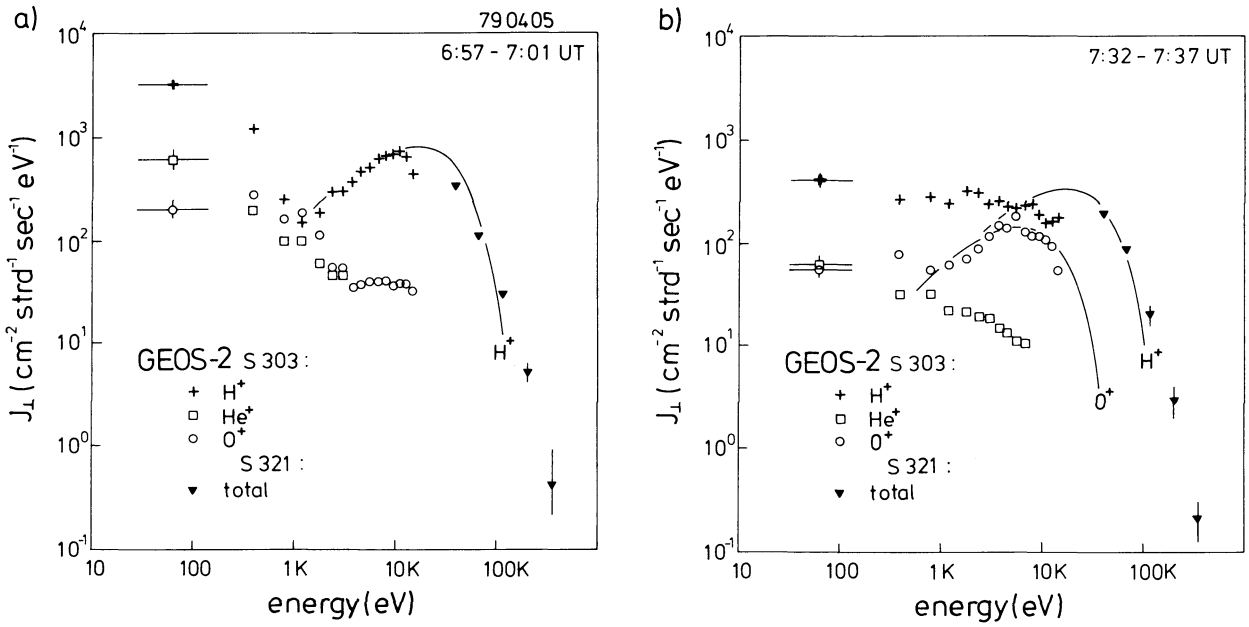

Fig. 6a and b. Ion fluxes perpendicular to the magnetic field, measured by the ICE mass spectrometer (experiment S-303, $E<16$ keV) and the CPS detector (experiment S-321, $E>27$ keV) on board GEOS-2. **a** Before and **b** after the start of the pc2 activity. For the dominant energetic ions, the fluxes of equivalent Maxwellian ion distributions have been drawn into the diagrams. Their parameters are in **a**: $N_{H^+}=2\ \mathrm{cm}^{-3}$, $T_{\perp H^+}=20$ keV; **b**: $N_{H^+}=0.6\ \mathrm{cm}^{-3}$, $N_{O^+}=0.8\ \mathrm{cm}^{-3}$, $T_{\perp H^+}=20$ keV, $T_{\perp O^+}=6$ keV. An anisotropy of 1 was assumed

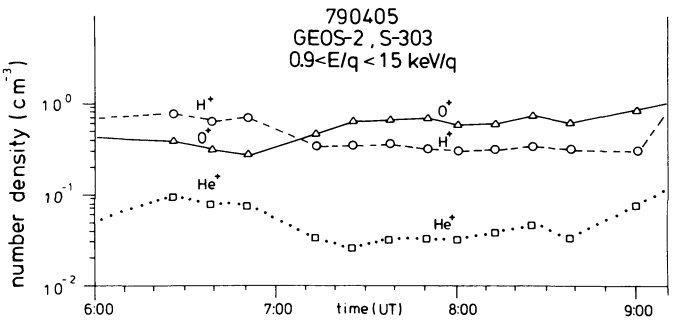

Fig. 7. Equivalent number densities of H^+, O^+ and He^+ ions in the energy range 0.9–16 keV/e. The densities are derived from the ion flux measurements of the ion composition experiment (S-303) under the assumption of thermal isotropy of the velocity distributions

321 particle detector for ion energies above 27 keV. This detector does not resolve the different ion species, but it is assumed that the ion flux at these energies is dominated by H^+. Figure 8 shows, as an example, the anisotropic ion flux at the time of large pc2 activity at 8:35 UT and its gradual increase from 8:05 UT, when no pc2 waves were recorded.

Admittedly, a bi-Maxwellian distribution function is not always a good model for energetic magnetospheric particles. While before 7:00 UT, for example, the energetic H^+ flux corresponds closely to a Maxwellian with a temperature $T_\perp \simeq 20$ keV and a density $N \simeq 2$ cm^{-3} (Fig. 6a), it considerably deviates from being a Maxwellian after 7:00 UT (Fig. 6b). The energetic O^+ flux in Fig. 6b can roughly be described by the parameters $T_\perp \simeq 6$ keV and $N \simeq 0.8\ \mathrm{cm}^{-3}$. However, at times we even observed slightly positive gradients $\partial g/\partial v_\perp$ of the O^+ distribution in the energy range 1–3 keV. Likewise, the values of 2–3 for the temperature ratio $T_\perp/T_\parallel$ of energetic H^+, that we derived from the two lowest energy channels of the S-321 experiment (see Fig. 8), are not quite consistent with its derivation from the maximum unstable frequency f_{m1} of the pc1 waves which, for a Maxwell distribution of the energetic H^+ ions, should be (e.g. Cupermann, 1981)

$$f_{m1} = \left(1 - \left(\frac{T_\parallel}{T_\perp}\right)_{H^+}\right) f_{H^+}.$$

The latter method always gave higher values for the anisotropy, which we attribute to a high energy tail in the H^+ distribution. It can considerably increase the maximum frequency f_{m1}, as has been demonstrated by Leubner (1983).

For the lower energies, the measured ion fluxes were rather small, inferring a number density of approximately 0.08, 0.05 and 0.01 cm^{-3} for H^+, O^+ and He^+ ions, respectively, in the energy range from 100–900 eV. The total ion number density, as derived from plasma frequency measurements on board GEOS-2, gave values of 7–10 cm^{-3} for the time of the pc2 events (Experiment S-301; Higel, personal communication). In order to calculate the dispersion relation (1), we therefore modelled the cold plasma by isotropic Maxwellians with various $H^+/O^+/He^+$ ratios under the constraint that the total ion density was 8 cm^{-3} and the cold plasma composition was not too different from that observed in the 100–900 eV energy range.

Figure 9 shows the calculated dispersion of the ion cyclotron waves propagating parallel to the magnetic field, when the parameters of the ion distributions were chosen in accord with the particle measurements. The observed pc1 and pc2 waves, partly visible in Fig. 2, are reproduced by the unstable frequency bands at

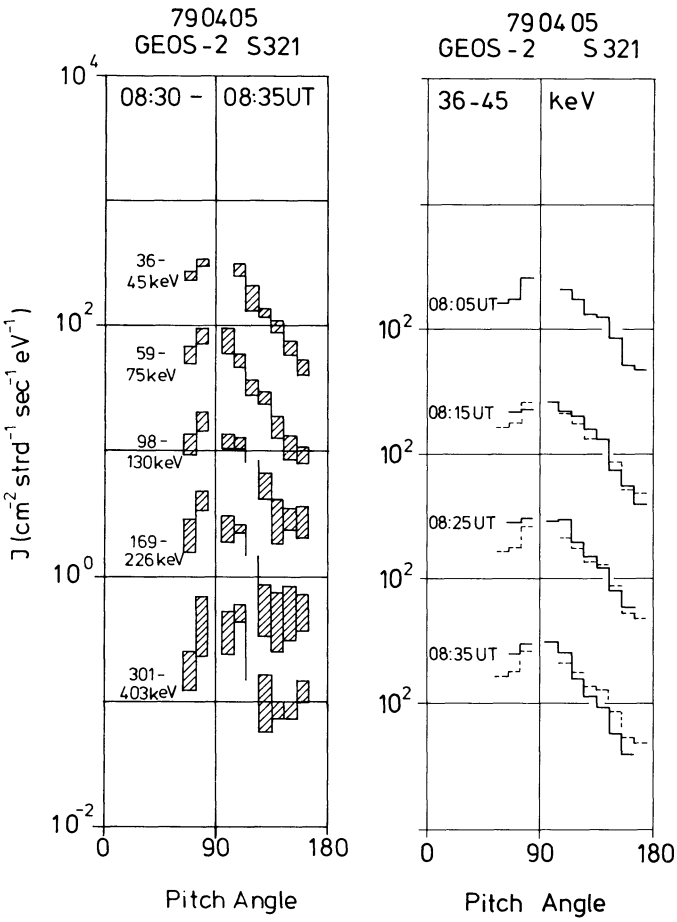

Fig. 8. Pitch-angle dependance of the energetic ion flux. The diagram on the left has been obtained by a superposition of the measurements between 8:30 and 8:35 UT. Unfortunately, there are still data gaps at some angles, in particular at $\alpha = 90°$ which is due to sunlight shining onto the detector. The diagram on the *right* shows the temporal evolution of the pitch angle variation of the ion flux in one of the energy channels from 8:05–8:35 UT. As reference, the ion flux at 8:05 UT is superimposed each time as a *hatched line*

$f \simeq 0.5 f_{H^+}$ and below f_{O^+} in Fig. 9. Undertermined from the measurements was the anisotropy of the energetic O^+ ions. However, it was found that in order to destabilize ion cyclotron waves below f_{O^+}, the O^+ anisotropy had to be comparable to that of the energetic H^+ ions.

The effect of various cold plasma compositions is also shown in Fig. 9. For a cold plasma temperature of 12 eV, a He^+ abundance above $\sim 5\%$ of the total density causes the appearance of an additional unstable frequency band just below f_{He^+} (dashed and dotted lines in Fig. 9). LH polarized waves at these frequencies are commonly observed on board GEOS-1 and 2 (Young et al., 1981; Roux et al., 1982), but they are absent in the ULF spectrum in Fig. 2, from which we conclude that the He^+ abundance was below 5% at that time. A higher cold plasma temperature, which would have damped these ion cyclotron waves below f_{He^+} even for higher He^+ abundances, must be excluded, since this would have caused an increased ion flux in the lowest energy channel in Fig. 6. In a similar calculation, which also takes account of the observed energetic He^+ ions, we found that they had only a negligible effect on the results of Fig. 9 of slightly lowering the growth rate at frequencies immediately below f_{He^+}.

From the results of Fig. 9 it is evident that a higher O^+ content of the cold plasma mainly causes the cut-off frequencies of the wave bands below f_{He^+} and f_{H^+} to move towards their adjacent gyrofrequencies, thus narrowing the frequency bands within which a propagation of ion cyclotron waves is possible (dashed lines in Fig. 9). Since the lowest unstable LH polarized pc1 frequency in the ULF spectrum was as high as 0.4–0.5 f_{H^+} (see Fig. 2), a cold O^+ abundance of between 20% and 30% had to be assumed.

Another consequence of the high O^+ abundance is a relatively large value for the cross-over frequency between f_{He^+} and f_{H^+}. From Fig. 9 we find that it is positioned within the unstable pc1 frequency band which can explain why the observed pc1 waves are not

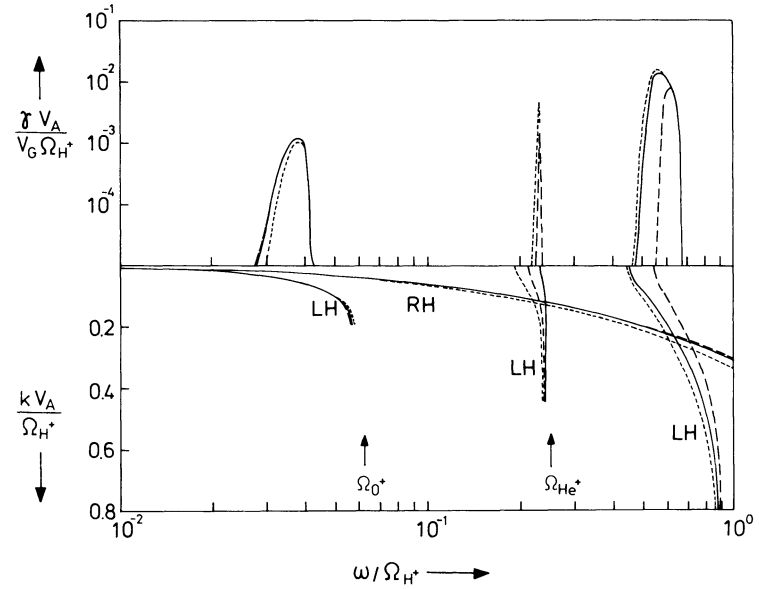

Fig. 9. Normalized convective growth rate (*top*) and normalized wave number (*bottom*) versus normalized wave frequency for LH polarized ion cyclotron waves propagating parallel to the magnetic field in a plasma composed of H^+, He^+ and O^+ ions. To indicate the various cross-over frequencies, the dispersion of the RH polarized mode is also given in the *lower panel*. The plasma was modelled by bi-Maxwellian distribution functions. The hot component parameters are $N_{H^+} = 0.6\,cm^{-3}$, $N_{O^+} = 0.8\,cm^{-3}$, $T_{\perp H^+} = 30\,keV$, $T_{\perp O^+} = 9\,keV$ and $T_\perp/T_\parallel = 3$ for both. The cold plasma is composed of isotropic Maxwellians with a temperature of 12 eV and various densities $N_{H^+}/N_{O^+}/N_{He^+}$: (*full line*) 4.2/2.2/0.2 cm^{-3}; (*dashed*) 3.5/2.5/0.6 cm^{-3}; (*dotted*) 4.5/1.5/0.6 cm^{-3}. A further parameter used in the calculation was the magnetic field $B = 200$ nT

simply polarized in the LH sense. Usually, the cross-over frequency is found just below the unstable pc1 frequencies at the equator, and a deviation from LH polarization is only observed after the pc1 waves have travelled some distance off the equator (Young et al., 1981; Fraser and McPherron, 1982).

Discussion

The calculations in the last section demonstrate that the observed amount of energetic O^+ ions is sufficient to destabilize ion cyclotron waves below f_{O^+}, provided a positive anisotropy of the O^+ distribution is assumed. It is very probable that the pc2 emission observed on GEOS-2 and simultaneously on the ground are such ion cyclotron waves, since they show the characteristic features of these waves, i.e. LH polarization, a small frequency band width and a close correlation of their frequency with f_{O^+}.

A different pc2 wave generation mechanism has been proposed recently by Lanzerotti et al. (1983) in order to explain pc2 waves with a peak-to-peak amplitude of almost 30 nT, which they observed at mid-latitude ground-based magnetometer stations. They related the wave period to the bounce period of 100 keV protons along the geomagnetic field line. A similar mechanism, however, cannot explain our observations at high geomagnetic latitudes since the bouncing ions then require an energy of almost 1 MeV in order to match the observed wave frequency.

It might be questioned, however, whether the growth rates, calculated from our model, are large enough to explain the observed amplitude of the pc2 waves, reaching some nT on the ground. The maximum convective growth rate for the pc2 waves was calculated to be $\gamma/V_G \simeq 10^{-3}\, \Omega_{H^+}/V_A$, where V_A and V_G are the Alfvén and group velocity respectively. Because of the small wave number $k \simeq 0.04\, \Omega_{H^+}/V_A$ of the pc2 waves, a typical change of their amplitude then occurs over about 10 wavelengths. Inspection of Fig. 1 shows that the amplitude modulation of the pc2 wave packets takes a couple of oscillations. This is in rough correspondence with the calculated growth rates under the assumption that the instability remains in its linear convective state. Under the assumed conditions, the Alfvén velocity is $V_A \simeq 600$ km/s so that 10 wavelengths correspond to roughly $8R_E$, which is probably longer than the extent of the wave generation region. It seems that good reflection conditions from the day-side ionosphere, causing the waves to bounce several times through the unstable region, are of great importance for the proposed pc2 generation.

On the other hand, higher growth rates would have easily been obtained if a high energetic tail of the ion distributions had been taken into account (Leubner, 1983). The O^+ ions which interact with the pc2 waves have a parallel velocity of about $0.6\, V_A$, corresponding to almost 10 times their mean parallel energy. A Maxwellian distribution may considerably underestimate the actual ion density at these energies. Furthermore, the anisotropy of the energetic O^+ ions was not measured directly but set equal to that of the energetic H^+ ions. A higher value for their anisotropy would also increase the growth rate. The contribution of energetic H^+ ions to the instability of the pc2 waves is very small, since the H^+ ions that resonate with these waves require a parallel velocity of $21.5\, V_A$, which is more than 100 times their mean parallel energy.

A still somewhat open question is, what actually controls the ion cyclotron wave activity? Clearly, the energetic O^+ ions that appear after 7:00 UT supply the free energy fed into the pc2 waves. However, as can be seen in Fig. 7, their density was not reduced between 7:40 and 8:30 UT, when no pc2 waves were recorded. Also, a change in the cold plasma density that can modulate ion cyclotron wave generation (Cornwall, 1976; Mauk and McPherron, 1980) was not seen. Since the maximum pc1 frequency f_{m1} was reduced between 8:00 and 8:30 UT, we conclude that the anisotropy of the energetic H^+ ions had decreased and, probably, the anisotropy of the energetic O^+ ions dropped below the threshold value. The pitch angle variation of the observed ion flux above 27 keV confirms this conclusion (see Fig. 8). However, the changes of the equivalent Maxwellian temperatures $T_\perp$, $T_\parallel$ derived from these data are smaller than expected from the wave observation.

Another interesting, but uninterpreted problem are the faint magnetosonic waves that sometimes became visible in the field-aligned component of the GEOS-2 wave measurements during the pc2 activity. Their frequency was near f_{He^+} and $1.5\, f_{H^+}$ and a wave magnetic field perpendicular to the ambient magnetic field could not be detected for these waves. We conclude that their wave vector is directed perpendicular to the field lines, similar to the magnetosonic waves at multiples of f_{H^+} which were observed by Perraut et al. (1982). They found that these waves were destabilized by a positive gradient $\partial g/\partial v_\perp$ of the H^+ velocity distribution, and at least one of the magnetosonic emissions observed in our case was preceded by the detection of a positive gradient $\partial g/\partial v_\perp$ of the O^+ velocity distribution at energies between 1 and 3 keV. However, an extension of the results of Perraut et al. (1982) to a plasma composed of several ion species is not straight-forward because, here, multiples of the various gyrofrequencies and the ion-ion hybrid frequencies are resonances for perpendicular propagation. In a plasma with an ion composition as found in our case, the $He^+ - H^+$ hybrid frequency is very close to f_{He^+}, which might be of importance for the magnetosonic waves recorded near f_{He^+}.

In conclusion, the present observation shows the drastic effects that an enhanced O^+ population in the magnetosphere can have on the ion cyclotron wave generation. Large O^+ densities during the main and recovery phase of a substorm are often observed by satellite mass spectrometers. Cold O^+ abundances have been reported by Geiss et al. (1978) and Horwitz et al. (1983) from GEOS and ISEE measurements outside the plasmasphere. During disturbed periods they find the O^+ density even in excess of the He^+ density for energies below 100 eV, corresponding to the outcome of our model calculations. The energetic O^+ fluxes were found both field-aligned (Shelley et al., 1972) and trapped (Johnson et al., 1977) but only seldom do they seem to have a sufficiently positive anisotropy at the magnetic equator to be able to destabilize ion cyclotron

waves. However, the differential drift of trapped energetic O^+ ions (Lennartsson et al., 1981) may, in some regions of the magnetosphere, led to O^+ distributions with positive anisotropy, as has been assumed to exist in the present study. That pc2 waves are only rarely observed could be due to the fact that a sufficient enhancement of $(T_\perp/T_\parallel)_{O^+}$ at the magnetic equator depends on several conditions which are not often met simultaneously.

Acknowledgements. The present work was initiated by O. Hillebrand. We thank R. Gendrin, C.A. Green, L.J. Lanzerotti and M. Lester for helpful communication during the preparation of the article. We are also grateful to B. Higel for providing data from the S-301 experiment on GEOS-2 and T. Bösinger for pulsation sonograms from Sodankylä (Finland).

References

Balsiger, H., Eberhardt, P., Geiss, I., Young, D.T.: Magnetic storm injection of 0.9 to 16 keV/e solar and terrestrial ions into the high altitude magnetosphere. J. Geophys. Res. **85**, 1645–1662, 1980

Bossen, M., McPherron, R.L., Russel, C.T.: Simultaneous pc1 observations by synchronous satellite ATS-1 and ground stations: implications concerning IPDP generation mechanisms. J. Atmosph. Terr. Phys. **38**, 1157–1167, 1976

Cornwall, J.M.: Cyclotron instabilities and electromagnetic emission in the ULF and VLF ranges. J. Geophys. Res. **70**, 61–69, 1965

Cornwall, J.M.: Density sensitive instabilities in the magnetosphere. J. Atmosph. Terr. Phys. **18**, 1111–1114, 1976

Cupermann, S.: Electromagnetic kinetic instabilities in multicomponent space plasmas: theoretical predictions and computer simulation experiments. Rev. Geophys. Space Phys. **19**, 307–343, 1981

Fraser, B.J., McPherron, R.L.: Pc1–2 magnetic pulsation spectra and heavy ion effects at synchronous orbit: ATS-6 results. J. Geophys. Res. **87**, 4560–4566, 1982

Geiss, I., Balsiger, H., Eberhardt, P., Walker, H.P., Weber, L., Young, D.T., Rosenbauer, H.: Dynamics of magnetospheric ion composition as observed by GEOS mass spectrometer. Space Sci. Rev. **22**, 537–566, 1978

Gendrin, R.: General relationships between wave amplification and particle diffusion in a magnetoplasma. Rev. Geophys. Space Phys. **19**, 171–184, 1981

Gendrin, R., Perraut, S., Fargetton, H., Glangeaud, F., Lacoume, J.L.: ULF waves: Conjugated ground satellite relationships. Space Sci. Rev. **22**, 433–442, 1978

Horwitz, J.L., Chappell, C.R., Reasoner, D.L., Craven, P.D., Green, J.L., Baugher, C.R.: Observations of low-energy plasma composition from the ISEE-1 and SCATHA satellites, in: R.G. Johnson (ed.), Energetic ion composition in the earth's magnetosphere. Terra Scientific Publ. Comp., Tokyo, 1983

Johnson, R.G., Sharp, R.D., Shelley, E.G.: Observations of ions of ionospheric origin in the storm time ring current. Geophys. Res. Lett. **4**, 403–406, 1977

Korth, A., Kremser, G., Wilken, B.: Observation of substorm associated particle flux variations at $6 < L < 8$ with GEOS-1. Space Sci. Rev. **22**, 501–509, 1978

Lanzerotti, L.J., Medford, L.V., Hasegawa, A., Lin, D.L.: Large amplitude ion bounce wave in the magnetosphere near L = 3. Geophys. Res. Lett. **10**, 479–481, 1983

Lennartsson, W., Sharp, R.D., Shelley, E.G., Johnson, R.G., Balsiger, H.: Ion composition and energy distribution during 10 magnetic storms. J. Geophys. Res. **86**, 4628–4638, 1981

Leubner, M.P.: High-energy tail distributions and resonant wave particle interaction. J. Geophys. Res. **88**, 469–473, 1983

Mauk, B.H.: Frequency gap formation in electromagnetic cyclotron wave distributions. Geophys. Res. Lett. **10**, 635–638, 1983

Mauk, B.H., McPherron, R.L.: An experimental test of the electromagnetic ion cyclotron instability within the earth's magnetosphere. Phys. Fluids **23**, 2111–2127, 1980

Perraut, S.: Wave particle interaction in the ULF range: GEOS-1 and -2 results. Planet. Space Sci. **30**, 1219–1227, 1982

Perraut, S., Gendrin, R., Robert, P., Roux, A., de Villedary, C., Jones, D.: ULF waves observed with magnetic and electric sensors on GEOS-1. Space Sci. Rev. **22**, 347–369, 1978

Perraut, S., Roux, A., Robert, P., Gendrin, R., Sauvaud, J.-A., Bosqued, J.-M., Kremser, G., Korth, A.: A systematic study of ULF waves above F_{H^+} from GEOS-1 and -2 measurements and their relationships with proton ring distributions. J. Geophys. Res. **87**, 6219–6236, 1982

Perraut, S., Gendrin, R., Roux, A., de Villedary, C.: Ion cyclotron waves: direct comparison between ground based measurements and observations in the source region. J. Geophys. Res. **89**, 195–202, 1984

Rauch, J.L., Roux, A.: Ray tracing of ULF waves in a multicomponent magnetospheric plasma: Consequences for the generation mechanism of ion cyclotron waves. J. Geophys. Res. **87**, 8191–8198, 1982

Roux, A., Perraut, S., Rauch, J.L., de Villedary, C., Kremser, G., Korth, A., Young, D.T.: Wave particle interactions near Ω_{He^+} observed on board GEOS-1 and -2, 2. Generation of ion cyclotron waves and heating of the He^+ ions. J. Geophys. Res. **87**, 8174–8190, 1982

Shelley, E.G., Sharp, R.D., Johnson, R.G.: Satellite observations of heavy ions during a geomagnetic storm. J. Geophys. Res. **77**, 6104–6110, 1972

Wedeken, U., Inhester, B., Korth, A., Glaßmeier, K.H., Gendrin, R., Lanzerotti, L.J., Gough, H., Green, C.A., Amata, E., Pedersen, A., Rostoker, G.: Ground-satellite coordinated study of the April 5, 1979 events: flux variation of energetic particles and associated magnetic pulsations. J. Geophys. **55**, 120–133, 1984

Young, D.T.: Heavy ion plasmas in the outer magnetosphere. J. Geophys. **52**, 167–175, 1983

Young, D.T., Perraut, S., Roux, A., de Villedary, C., Gendrin, R., Korth, A., Kremser, G., Jones, D.: Wave particle interactions near Ω_{He^+} observed on GEOS-1 and -2, 1. Propagation of ion cyclotron waves in a He^+ rich plasma. J. Geophys. Res. **86**, 6755–6772, 1981

Received November 24, 1983; Revised version March 19, 1984
Accepted March 21, 1984